A Simple and Rigorous Analysis of the Transmission Properties of a Sector Horn Junction in a Rectangular Waveguide

Takashi Tsushima, Shuzo Kuwano, *Member, IEEE,* and Kinchi Kokubun, *Member, IEEE*

Abstract—**Rigorous representations of expansion with a modal function, reflection and transmission coefficients for the electromagnetic field at the junction between a sector horn and a rectangular waveguide are obtained. So far, this problem has been approximately treated by limiting the mode number of the electromagnetic field expansion or the flare angle of the horn. In this paper, the electromagnetic fields at the discontinuity are expanded by a modal function of integer order. As a result, rigorous solutions are simply obtained by the orthogonality of a trigonometric function without any qualification. By using the numerical results with strict accuracy calculated from these representations, the transmission properties at the junction between a sector horn and a rectangular waveguide are examined in detail.**

I. Introduction

THE transmission properties of a sector horn junction in a rectangular waveguide are a basic problem of elements in microwave hardware. Finding the exact solution of the sector horn's properties is important for appreciating the limit on the generation of higher order modes in the sector horn junction, because the quantities of higher order modes generated in the sector horn junction are larger than in horns with a continuous curvilinear taper [1]–[3].

In former theoretical studies [4]–[6] of the guide-to-taper junction, some conditions have been attached to modal expansions of the electromagnetic fields on such a junction and the flare angles. In [7] Piefke analyzes the properties of the junction by taking account of higher order modes, but deals only with horns in which the flare angle is small. Recently a taper to connect waveguides of different diameters has been solved accurately by the technique of cascading scattering matrices and the coupled wave equations [8], but the junction between a semi-infinite waveguide and a horn [9] cannot be treated by these methods. On the other hand, Lewin [10] suggests a rigorous representation to the tapered guide section but does not derive the solution. Though a full numerical analysis based on the finite-element method [11] is very useful, the computing procedures are onerous.

The sector horn, whose configuration is very simple, is used so widely that it is desirable to have its properties clarified easily by applying simple expressions. In this paper transmission properties of an E-plane and an H-plane sector horn junction in a rectangular waveguide are analyzed without restricting the flare angles, the modal expansions of the electromagnetic fields, etc. Moreover, with the modal functions of the field expansion, simple expressions of the reflection and transmission coefficients are simply derived. By using these expressions, the transmission properties of the junction are clarified in numerical values which are very accurate.

Manuscript received March 22, 1990; revised September 4, 1990.

T. Tsushima was with the Department of Electrical Engineering, Nihon University, Fukushima, Japan. He is now with the Aomori Technical High School, Aomori-shi, Aomori 038, Japan.

S. Kuwano and K. Kokuban are with the Department of Electrical Engineering, Nihon University, Koriyama-shi, Fukushima 963, Japan.

IEEE Log Number 9041069.

II. Properties of an E-Plane Sector Horn Junction

A. The Electromagnetic Fields of Each Region

Fig. 1 shows the structure and coordinate systems of the junction between an E-plane sector horn with a flare angle ϕ_0 and a rectangular waveguide which has width a and height b. The incident wave of TE_{10} mode propagating in region I of the waveguide is reflected at the discontinuous section and is transmitted to the horn section of region III, which is to the right of the arc ACB of the circle centered on 0′. The fields of regions I and III are expanded in the rectangular coordinate system (x, y, z) and the cylindrical coordinate system $(r_{\mathrm{III}}, \phi_{\mathrm{III}}, x')$, respectively. The fields of region II (segment ABC) are expanded in the cylindrical coordinate system $(r_{\mathrm{II}}, \phi_{\mathrm{II}}, x'')$. The fields of region I and others are represented to the modal function of LSE_{1m} and TE mode, respectively.

In region I, the field expansion is

$$H_x^{\mathrm{I}} = A_{10}^{i} \sin\frac{\pi}{a}x e^{-j\beta_{10}^{\mathrm{I}}z} + \sum_{m=0}^{\infty} A_{1m} \sin\frac{\pi}{a}x \cos\frac{m\pi}{b}\left(y+\frac{b}{2}\right)e^{j\beta_{1m}^{\mathrm{I}}z}, \quad m = 0,2,4,\cdots \tag{1}$$

where

$$k = \omega\sqrt{\varepsilon_0\mu_0}$$

$$k_{c1m}^{\mathrm{I}} = \sqrt{\left(\frac{\pi}{a}\right)^2 + \left(\frac{m\pi}{b}\right)^2}$$

$$\beta_{1m}^{\mathrm{I}} = \sqrt{k^2 - \left(k_{c1m}^{\mathrm{I}}\right)^2}.$$

In region II, because of being contained within the circle with a center 0 and a radius $b/2$, the field is expanded to

0018-9480/91/0200-0287$01.00 ©1991 IEEE

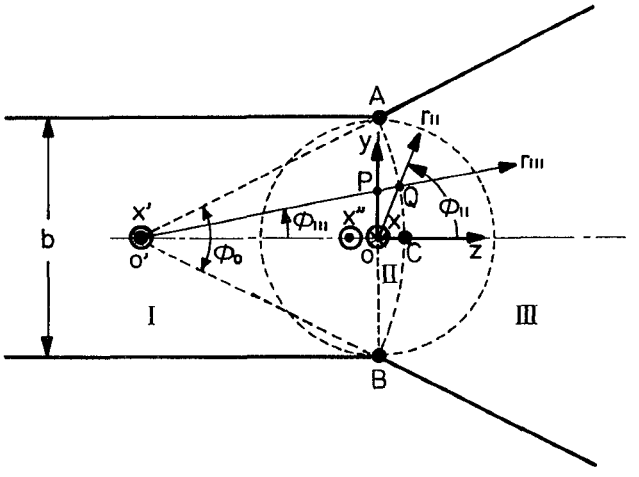

Fig. 1. E-plane sector horn junction in a rectangular waveguide and coordinate systems.

the modal function of integer n as follows:

$$H_{x''}^{\mathrm{II}} = \sum_{n=0}^{\infty} C_n J_n\left(k_c^{\mathrm{II}} r_{\mathrm{II}}\right) \cos n\phi_{\mathrm{II}} \sin \frac{\pi}{a} x'', \qquad n = 0,1,2,\cdots \tag{2}$$

where $k_c^{\mathrm{II}} = \sqrt{k^2 - (\pi/a)^2}$.

In region III, the field expansion is

$$H_{x'}^{\mathrm{III}} = \sum_{n=0}^{\infty} B_n H_\nu^{(2)}\left(k_c^{\mathrm{III}} r_{\mathrm{III}}\right) \cos \nu\phi_{\mathrm{III}} \sin \frac{\pi}{a} x', \tag{3}$$

where $k_c^{\mathrm{III}} = \sqrt{k^2 - (\pi/a)^2}$ and $\nu = 2n\pi/\phi_0$. From expressions (1)–(3), the rest of the field components in region I, II, and III, that is, $(E_y^{\mathrm{I}}, E_z^{\mathrm{I}}, H_y^{\mathrm{I}}, H_z^{\mathrm{I}})$, $(E_{r\mathrm{II}}^{\mathrm{II}}, E_{\phi\mathrm{II}}^{\mathrm{II}}, H_{r\mathrm{II}}^{\mathrm{II}}, H_{\phi\mathrm{II}}^{\mathrm{II}})$, and $(E_{r\mathrm{III}}^{\mathrm{III}}, E_{\phi\mathrm{III}}^{\mathrm{III}}, H_{r\mathrm{III}}^{\mathrm{III}}, H_{\phi\mathrm{III}}^{\mathrm{III}})$, are derived, respectively. In expressions (1)–(3), ω, ε_0, and μ_0 are the angular frequency, the permittivity, and the permeability in free space, respectively. Also, J_n is the Bessel function of the first kind of nth order and $H_\nu^{(2)}$ is the Hankel function of the second kind of νth order. A_{10}^t, A_{1m}, B_n, and C_n are the amplitudes of the modal functions.

B. The Amplitudes of the Modal Functions

The boundary conditions of the electromagnetic fields in regions I, II, and III are as follows. The boundary conditions at point P on the boundary AB are

$$E_y^{\mathrm{I}} = E_{r\mathrm{II}}^{\mathrm{II}} \qquad -H_x^{\mathrm{I}} = H_{x''}^{\mathrm{II}}. \tag{4}$$

Similarly, at point Q in the boundary ACB,

$$\left.\begin{aligned} &E_{r\mathrm{II}}^{\mathrm{II}} \sin\left(\phi_{\mathrm{II}} - \phi_{\mathrm{III}}\right) + E_{\phi\mathrm{II}}^{\mathrm{II}} \cos\left(\phi_{\mathrm{II}} - \phi_{\mathrm{III}}\right) = E_{\phi\mathrm{III}}^{\mathrm{III}} \\ &H_{x''}^{\mathrm{II}} = H_{x'}^{\mathrm{III}}. \end{aligned}\right\} \tag{5}$$

Equations (4) and (5) yield the following expressions for the amplitudes C_n, A_{1m}, and B_n of each modal function:

$$[C_n] = \begin{bmatrix} P_{pq} \\ Q_{pq} \end{bmatrix}^{-1} [A^t], \qquad [A^t] = \left[-2A_{10}^t, 0, 0, \cdots, 0\right]^T \tag{6}$$

where

$$\left.\begin{aligned} P_{pq} &= -\frac{R_{pq}}{2} \\ &\quad - j\frac{2\left\{k_{c(2p-2)}^{\mathrm{I}}\right\}^2}{k_c^{\mathrm{II}} \beta_{(2p-2)}^{\mathrm{I}} b} \int_0^{b/2} \frac{q-1}{k_c^{\mathrm{II}} y_1} J_{q-1}\left(k_c^{\mathrm{II}} y_1\right) \\ &\quad \cdot \cos\frac{\pi}{2} q \cos\frac{2(p-1)\pi}{b}\left(y_1 + \frac{b}{2}\right) dy_1 \\ Q_{pq} &= \frac{\phi_0 H_{\nu(p-1)}^{(2)\prime}\left(k_c^{\mathrm{III}} r_{\mathrm{III}}'\right)}{4} T_{pq} \\ &\quad - 2\int_0^{\phi_0/2} \left\{ \frac{q-1}{k_c^{\mathrm{II}} r_{\mathrm{II}}'} J_{q-1}\left(k_c^{\mathrm{II}} r_{\mathrm{II}}'\right) \sin\left(q-1\right)\phi_{\mathrm{II}}' \right. \\ &\quad \cdot \sin\left(\phi_{\mathrm{II}}' - \phi_{\mathrm{III}}\right) + J_{q-1}'\left(k_c^{\mathrm{II}} r_{\mathrm{II}}'\right) \\ &\quad \left. \cdot \cos\left(q-1\right)\phi_{\mathrm{II}}' \cos\left(\phi_{\mathrm{II}}' - \phi_{\mathrm{III}}\right) \right\} \\ &\quad \cdot \cos\frac{2(p-1)\pi}{\phi_0} \phi_{\mathrm{III}}\, d\phi_{\mathrm{III}} \end{aligned}\right\} \tag{7}$$

$$\left.\begin{aligned} R_{pq} &= -\frac{4\left\{k_{c(2p-2)}^{\mathrm{I}}\right\}^2}{\left\{k^2 - \left(\frac{\pi}{a}\right)^2\right\} b} \int_0^{b/2} J_{q-1}\left(k_c^{\mathrm{II}} y_1\right) \sin\frac{\pi}{2} q \\ &\quad \cdot \cos\frac{2(p-1)\pi}{b}\left(y_1 + \frac{b}{2}\right) dy_1 \\ T_{pq} &= \frac{4}{\phi_0 H_{\nu(p-1)}^{(2)}\left(k_c^{\mathrm{III}} r_{\mathrm{III}}'\right)} \int_0^{\phi_0/2} J_{q-1}\left(k_c^{\mathrm{II}} r_{\mathrm{II}}'\right) \\ &\quad \cdot \cos\left(q-1\right)\phi_{\mathrm{II}}' \cos\frac{2(p-1)\pi}{\phi_0} \phi_{\mathrm{III}}\, d\phi_{\mathrm{III}} \end{aligned}\right\} \tag{8}$$

$$\left.\begin{aligned} &r_{\mathrm{II}}' = s r_{\mathrm{III}}' \qquad r_{\mathrm{III}}' = \frac{b}{2\sin\frac{\phi_0}{2}} \qquad \phi_{\mathrm{II}}' = \sin^{-1}\frac{\sin\phi_{\mathrm{III}}}{s} \\ &s = \sqrt{\sin^2\phi_{\mathrm{III}} + \left(\cos\phi_{\mathrm{III}} - \cos\frac{\phi_0}{2}\right)^2} \\ &k_{c(2p-2)}^{\mathrm{I}} = \sqrt{\left(\frac{\pi}{a}\right)^2 + \left\{\frac{2(p-1)\pi}{b}\right\}^2} \\ &\beta_{(2p-2)}^{\mathrm{I}} = \sqrt{k^2 - \left\{k_{c(2p-2)}^{\mathrm{I}}\right\}^2} \end{aligned}\right\} \tag{9}$$

$$\nu(p-1) = \frac{2(p-1)\pi}{\phi_0}$$

$$\left.\begin{aligned} &n = 0,1,2,\cdots,t \\ &p = 1,2,3,\cdots,(t+1)/2 \\ &q = 1,2,3,\cdots,(t+1) \end{aligned}\right\} \quad \text{for } t \text{ odd.}$$

Also,

$$\left.\begin{aligned} A_{1m} &= A_{1m}', && m \neq 0 \\ A_{10} &= A_{10}'/2 - A_{10}', && m = 0 \end{aligned}\right\} \tag{10}$$

$$\left.\begin{aligned} B_n &= B_n', && n \neq 0 \\ B_0 &= B_0'/2, && n = 0 \end{aligned}\right\} \tag{11}$$

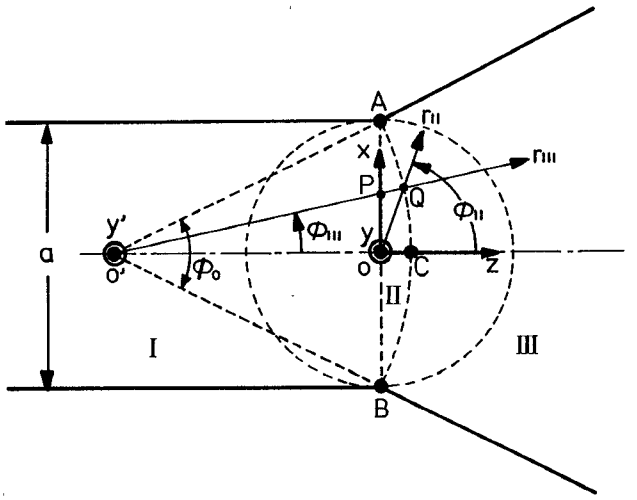

Fig. 2. *H*-plane sector horn junction in a rectangular waveguide and coordinate systems.

where

$$\left.\begin{aligned}[A'_{1m}] &= [R_{pq}][C_n] \\ [B'_n] &= [T_{pq}][C_n]\end{aligned}\right\} \tag{12}$$

$$\left.\begin{aligned}m &= 0,2,4,\cdots,2t \\ n &= 0,1,2,\cdots,t \\ p &= 1,2,3,\cdots,(t+1)\end{aligned}\right\} \quad \text{for } t \text{ odd.}$$

C. The Power Reflection and Transmission Coefficients

From expressions (10) and (11), the power reflection and transmission coefficients, that is, R_m and T_n, are

$$\left.\begin{aligned}R_0 &= R'_0, \quad m = 0 \\ R_m &= 2R'_m, \quad m \neq 0\end{aligned}\right\} \tag{13}$$

$$\left.\begin{aligned}T_0 &= T'_0/2, \quad m = 0 \\ T_n &= T'_n, \quad m \neq 0\end{aligned}\right\} \tag{14}$$

where

$$\left.\begin{aligned}R'_m &= \frac{\beta^{\mathrm{I}}_{1m}}{\beta^{\mathrm{I}}_{10}}\left(\frac{k^{\mathrm{I}}_{c10}}{k^{\mathrm{I}}_{c1m}}\right)^4\left|\frac{A_{1m}}{A'_{10}}\right|^2 \\ T'_n &= \frac{\phi_0\left(k^{\mathrm{I}}_{c10}\right)^4}{\pi\left(k^{\mathrm{III}}_c\right)^2\beta^{\mathrm{I}}_{10}\left\{k^2-\left(\frac{\pi}{a}\right)^2\right\}b}\left|\frac{B_n}{A'_{10}}\right|^2\end{aligned}\right\}. \tag{15}$$

If the number t of terms in the modal expansions in each region is increased, the accuracy of R_m and T_n is improved. R_m and T_n are satisfied with the condition of the following expression:

$$\left[R_0+\sum_{m=2}^{\infty}R_m\right]+\left[T_0+\sum_{n=1}^{\infty}T_n\right]=1. \tag{16}$$

III. Properties of an *H*-Plane Sector Horn Junction

Fig. 2 shows the structure and coordinate systems of the junction between an *H*-plane sector horn with a flare angle ϕ_0 and a rectangular waveguide of width a. The electromagnetic fields in regions I, II, and III are represented by the coordinate systems (x, y, z), $(r_{\mathrm{II}}, \phi_{\mathrm{II}}, y)$, and $(r_{\mathrm{III}}, \phi_{\mathrm{III}}, y')$, respectively. The fields in region I and the others are expanded in terms of TE and TM modal function.

In region I, the expansion of the modal function is

$$H^{\mathrm{I}}_z = A'_1\cos\frac{\pi}{a}\left(x+\frac{a}{2}\right)e^{-j\beta^{\mathrm{I}}_1 z} + \sum_{m=1}^{\infty}A_m\cos\frac{m\pi}{a}\left(x+\frac{a}{2}\right)e^{j\beta^{\mathrm{I}}_m z} \tag{17}$$

where $m = 1,3,5,\cdots$ and $\beta^{\mathrm{I}}_m = \sqrt{k^2-(m\pi/a)^2}$.

Similarly, in region II,

$$E^{\mathrm{II}}_y = \sum_{n=0}^{\infty}C_n J_n\left(k^{\mathrm{II}}_c r_{\mathrm{II}}\right)\cos n\phi_{\mathrm{II}} \tag{18}$$

and in region III,

$$E^{\mathrm{III}}_{y'} = \sum_{n=0}^{\infty}B_n H^{(2)}_{\nu}\left(k^{\mathrm{III}}_c r_{\mathrm{III}}\right)\cos\nu\phi_{\mathrm{III}} \tag{19}$$

where $n = 0,1,2,\cdots$, $k^{\mathrm{II}}_c = k^{\mathrm{III}}_c = k$, and $\nu = (2n+1)\pi/\phi_0$. In expressions (17)–(19), A'_1, A_m, B_n, and C_n are the amplitudes of the modal functions. By using expressions (17)–(19), the field components in each region, $(E^{\mathrm{I}}_y, H^{\mathrm{I}}_x)$, $(E^{\mathrm{II}}_{r\mathrm{II}}, E^{\mathrm{II}}_{\phi\mathrm{II}}, H^{\mathrm{II}}_{r\mathrm{II}}, H^{\mathrm{II}}_{\phi\mathrm{II}})$, and $(E^{\mathrm{III}}_{r\mathrm{III}}, E^{\mathrm{III}}_{\phi\mathrm{III}}, H^{\mathrm{III}}_{r\mathrm{III}}, H^{\mathrm{III}}_{\phi\mathrm{III}})$, are derived. Accordingly, the amplitudes C_n, A_m, and B_n and the power reflection and transmission coefficients are derived along lines very similar to the technique of the previous section.

The amplitudes C_n, A_m, and B_n are

$$[C_n] = \begin{bmatrix}P_{pq} \\ Q_{pq}\end{bmatrix}^{-1}[A^i], \qquad [A^i] = \left[-A'_1, 0, 0, \cdots, 0\right]^T \tag{20}$$

$$\left.\begin{aligned}A_1 &= A'_1 + A'_1, \quad m = 1 \\ A_m &= A'_m, \quad m \neq 1\end{aligned}\right\} \quad \text{for } [A'_m] = [R_{pq}][C_n] \tag{21}$$

$$[B_n] = [T_{pq}][C_n] \tag{22}$$

where $m = 1, 3, 5, \cdots, (2t+1)$, $n = 0, 1, 2, \cdots, t$, $p = 1,2,3,\cdots,(t+1)$, and t is an odd number. Also, the elements in the matrix of each expression, P_{pq}, Q_{pq}, R_{pq}, and

T_{pq}, are

$$\left.\begin{aligned} P_{pq} &= -\frac{2k^{\mathrm{I}}_{c(2p-1)}\omega\varepsilon_0}{k_c^{\mathrm{II}}\beta^{\mathrm{I}}_{(2p-1)}a} \\ &\cdot\int_0^{a/2}\frac{q-1}{k_c^{\mathrm{II}}x_1}J_{q-1}(k_c^{\mathrm{II}}x_1)\cos\frac{\pi}{2}q\sin\frac{(2p-1)\pi}{a}\left(x_1+\frac{a}{2}\right)dx_1 \\ Q_{pq} &= \frac{\phi_0 H^{(2)\prime}_{\nu(p-1)}(k_c^{\mathrm{III}}r'_{\mathrm{III}})}{4}T_{pq} \\ &\quad -2\int_0^{\phi_0/2}\left\{\frac{q-1}{k_c^{\mathrm{II}}r'_{\mathrm{II}}}J_{q-1}(k_c^{\mathrm{II}}r'_{\mathrm{II}})\right. \\ &\quad \cdot\sin(q-1)\phi'_{\mathrm{II}}\sin(\phi'_{\mathrm{II}}-\phi_{\mathrm{III}}) \\ &\quad \left.+J'_{q-1}(k_c^{\mathrm{II}}r'_{\mathrm{II}})\cos(q-1)\phi'_{\mathrm{II}}\cos(\phi'_{\mathrm{II}}-\phi_{\mathrm{III}})\right\} \\ &\quad \cdot\cos\frac{(2p-1)\pi}{\phi_0}\phi_{\mathrm{III}}\,d\phi_{\mathrm{III}} \end{aligned}\right\} \tag{23}$$

$$\left.\begin{aligned} R_{pq} &= j\frac{4k^{\mathrm{I}}_{c(2p-1)}}{\omega\mu_0 a}\int_0^{a/2}J_{q-1}(k_c^{\mathrm{II}}x_1)\sin\frac{\pi}{2}q \\ &\quad \cdot\sin\frac{(2p-1)\pi}{a}\left(x_1+\frac{a}{2}\right)dx_1 \\ T_{pq} &= \frac{4}{\phi_0 H^{(2)}_{\nu(p-1)}(k_c^{\mathrm{III}}r'_{\mathrm{III}})}\int_0^{\phi_0/2}J_{q-1}(k_c^{\mathrm{II}}r'_{\mathrm{II}}) \\ &\quad \cdot\cos(q-1)\phi'_{\mathrm{II}}\cos\frac{(2p-1)\pi}{\phi_0}\phi_{\mathrm{III}}\,d\phi_{\mathrm{III}} \end{aligned}\right\} \tag{24}$$

where

$$\left.\begin{aligned} &r'_{\mathrm{II}} = sr'_{\mathrm{III}} \qquad r'_{\mathrm{III}} = \frac{a}{2\sin\frac{\phi_0}{2}} \qquad \phi'_{\mathrm{II}} = \sin^{-1}\frac{\sin\phi_{\mathrm{III}}}{s} \\ &s = \sqrt{\sin^2\phi_{\mathrm{III}}+\left(\cos\phi_{\mathrm{III}}-\cos\frac{\phi_0}{2}\right)^2} \\ &k^{\mathrm{I}}_{c(2p-1)} = \frac{(2p-1)\pi}{a} \qquad \beta^{\mathrm{I}}_{(2p-1)} = \sqrt{k^2-\left\{k^{\mathrm{I}}_{c(2p-1)}\right\}^2} \\ &\nu(p-1) = \frac{(2p-1)\pi}{\phi_0} \end{aligned}\right\} \tag{25}$$

and

$$\left.\begin{aligned} &n = 0,1,2,\cdots,t \\ &p = 1,2,3,\cdots,(t+1)/2 \\ &q = 1,2,3,\cdots,(t+1) \end{aligned}\right\} \quad \text{for } t \text{ odd.}$$

Also, the power reflection and transmission coefficients, R_m and T_n, are

$$\left.\begin{aligned} R_m &= \frac{1}{m^2}\frac{\beta^{\mathrm{I}}_m}{\beta^{\mathrm{I}}_1}\left|\frac{A_m}{A^i_1}\right|^2 \\ T_n &= \frac{2\pi\phi_0}{Z_0^2(ka)^2\beta^{\mathrm{I}}_1 a}\left|\frac{B_n}{A^i_1}\right|^2, \qquad Z_0 = \sqrt{\frac{\mu_0}{\varepsilon_0}} \end{aligned}\right\} \tag{26}$$

R_m and T_n must satisfy the following expression:

$$\sum_{m=1}^{\infty}R_m + \sum_{n=0}^{\infty}T_n = 1. \tag{27}$$

IV. Numerical Results

It is difficult to solve analytically the integrals of (7), (8), (23), and (24), so we used a numerical integral technique called the Clenshaw–Curtis method where an absolute and a relative error are chosen to be zero.

Tables I and II show the convergence of R_m and T_n versus the number N of terms of the modal expansions in each region for the E-plane and H-plane sector horns. These values are computed by using the parameters of normalized frequency $ka/\pi = 1.5$, where k is the wavenumber in free space, a flare angle $\phi_0 = 70°$, and, particularly for the case of an E-plane sector horn with the size of the rectangular waveguide at $a = 2b$. (R_0, T_0, T_2, T_4) and (R_1, T_1, T_3, T_5) for the E-plane and H-plane sector horns are the power reflection coefficient of the dominant mode and the power transmission coefficient of higher order modes, respectively. $G_E = R_0 + T_0 + T_2 + T_4$ and $G_H = R_1 + T_1 + T_3 + T_5$ express how far expressions (16) and (27) are satisfied. For $N = 20$, T_0 and T_1 converge to nearly four decimal places; moreover, G_E and G_H converge to nearly five decimal places. Therefore, expressions (16) and (27) are well satisfied.

Figs. 3 and 4 show the frequency properties of the power reflection and transmission coefficients for an E-plane and an H-plane sector horn junction. In the characteristic curves shown in Fig. 3(a) and Fig. 4(a), the constricted parts are observed at $ka/\pi = (1.7, 6.5)$ for the E plane and (3.0, 5.0) for the H plane. There is a constriction yield because the reflected waves of higher order modes are excited in the rectangular waveguide at each ka/π as shown in Fig. 3(b) and (c) and Fig. 4(b) and (c). T_0 and T_1 decrease with the increase of flare angle ϕ_0, as shown in Fig. 3(a) and Fig. 4(a), but (T_2, T_4) and (T_3, T_5) increase as shown in Fig. 3(b) and (c) and Fig. 4(b) and (c). In $ka/\pi < 2.0$, if the flare angle is below about 120°, T_2 and T_3 are neglected for both junctions because they are below -25 dB. Therefore, we can treat these models by considering the dominant mode only. For example, at $ka/\pi = 1.5$ and $\phi_0 = 120°$, the power transmission coefficients are $T_0 = 0.9461$, $T_2 = 0.93\times10^{-4}$, and $T_4 = 0.45\times10^{-10}$ for the case of an E-plane sector horn and $T_1 = 0.9957$, $T_3 = 0.011$, and $T_5 = 0.49\times10^{-7}$ for the case of an H-plane sector horn. But if ka/π is not less than 2.0 and the flare angle increases, (T_2, T_4) and (T_3, T_5) cannot be neglected. For example, at $ka/\pi = 4.5$ and $\phi_0 = 90°$, the power transmission coefficients are $T_0 = 0.8240$, $T_2 = 0.1627$, and $T_4 = 0.56\times10^{-4}$ for the case of an E-plane sector horn and $T_1 = 0.8658$, $T_3 = 0.1313$, and $T_5 = 0.0029$ for an H-plane sector horn. These values are computed at $N = 12$ and satisfied in the extent of error below 0.1%. (R_0, R_2, R_4) and (R_1, R_3, R_5) increase with an increase in ϕ_0, and for $ka/\pi > 2.0$ (R_1, R_3, R_5) not only vary in complicated fashion but also reach minima at specific points.

In Fig. 5, for the power reflection coefficient of the dominant mode in the case of an E-plane sector horn, the results obtained here are compared with the results of [4], for which the parameters are $\phi_0 = 24°$ and $a = 2.25b$. There is agreement between the two. A certain discrepancy results from using the approximate formula for dominant mode and small flare angle in [4].

TABLE I
THE CONVERGENCE PROPERTIES OF THE POWER REFLECTION AND TRANSMISSION COEFFICIENTS WITH RESPECT TO THE NUMBER N OF TERMS IN THE EXPANSION OF THE MODAL FUNCTION FOR AN E-PLANE SECTOR HORN JUNCTION ($ka/\pi = 1.5$, $\phi_0 = 70°$, $a = 2b$)

N	R_0 ($\times 10^{-1}$)	T_0	T_2 ($\times 10^{-6}$)	T_4 ($\times 10^{-17}$)	G_E
4	0.2364	0.976170	0.2846	0.980	0.999813
8	0.2336	0.976615	0.2985	0.323	0.999979
12	0.2332	0.976668	0.3005	0.330	0.999994
16	0.2331	0.976684	0.3011	0.332	0.999997
20	0.2330	0.976690	0.3014	0.333	0.999998

TABLE II
THE CONVERGENCE PROPERTIES OF THE POWER REFLECTION AND TRANSMISSION COEFFICIENTS WITH RESPECT TO THE NUMBER N OF TERMS IN EXPANSION OF THE MODAL FUNCTION FOR AN H-PLANE SECTOR HORN JUNCTION ($ka/\pi = 1.5$, $\phi_0 = 70°$)

N	R_1 ($\times 10^{-2}$)	T_1	T_3 ($\times 10^{-4}$)	T_5 ($\times 10^{-12}$)	G_H
4	0.16953	0.992784	0.14846	0.8969	0.994494
8	0.18939	0.997838	0.13251	0.3045	0.999745
12	0.19075	0.998027	0.13175	0.2975	0.999947
16	0.19113	0.998057	0.13154	0.2958	0.999982
20	0.19128	0.998066	0.13146	0.2952	0.999992

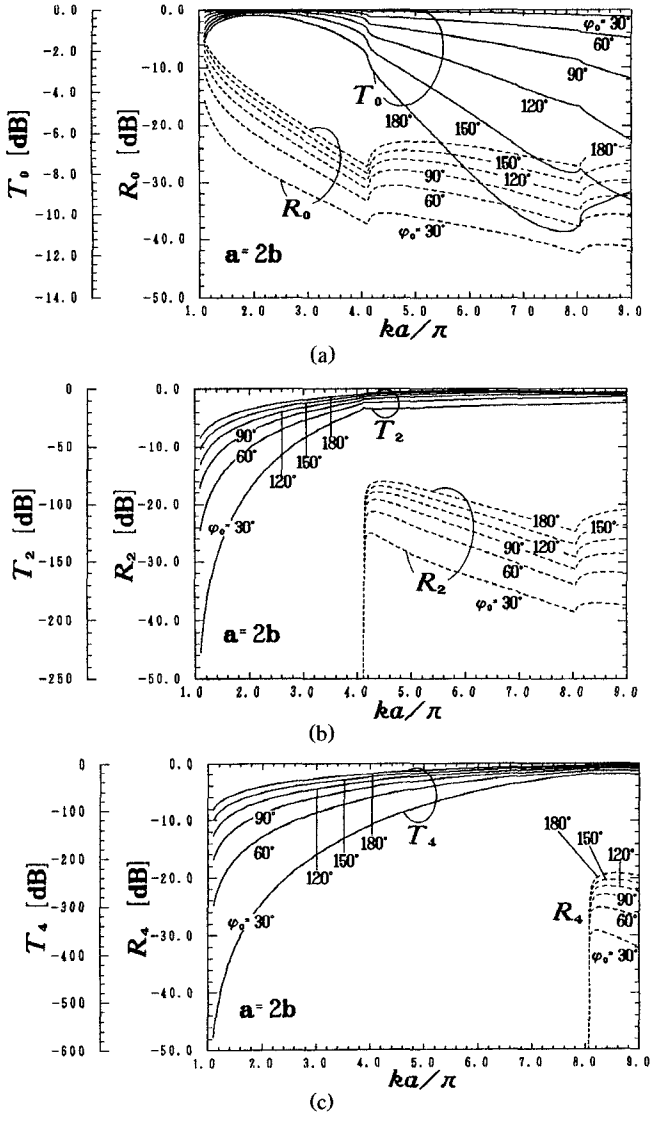

Fig. 3. Frequency properties of the power reflection and transmission coefficients for the case of an E-plane sector horn. (a) Properties of R_0 and T_0. (b) Properties of R_2 and T_2. (c) Properties of R_4 and T_4.

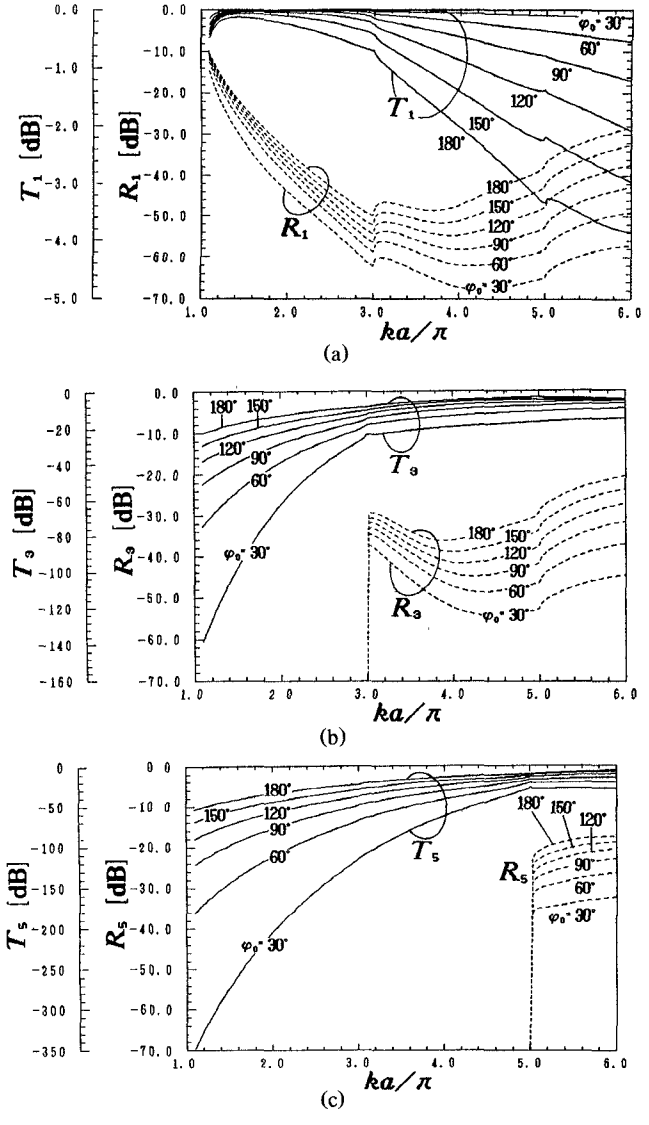

Fig. 4. Frequency properties of the power reflection and transmission coefficients for the case of an H-plane sector horn. (a) Properties of R_1 and T_1. (b) Properties of R_3 and T_3. (c) Properties of R_5 and T_5.

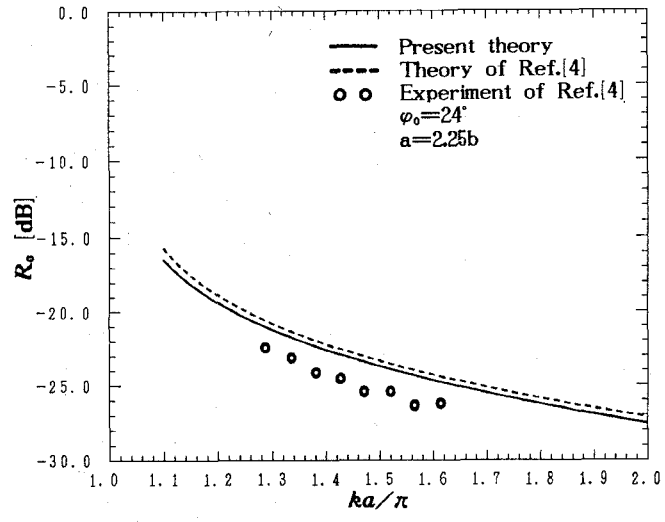

Fig. 5. Comparison between the results in this paper and in [4] with respect to the power reflection coefficient of the dominant mode for the case of an E-plane sector horn.

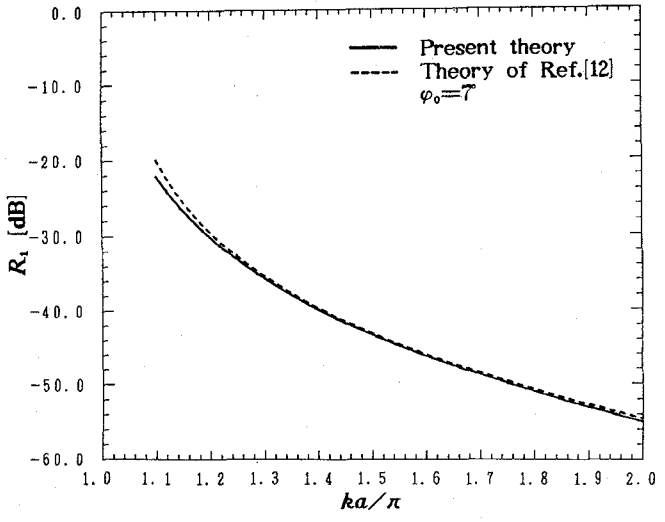

Fig. 6. Comparison between the results in this paper and in [12] with respect to the power reflection coefficient of the dominant mode for the case of an H-plane sector horn.

Similarly, the curves comparing the results in this paper with the results in [12] for an H-plane sector horn are shown in Fig. 6, for which the flare angle is $\phi_0 = 7°$. As ka/π approaches the cutoff frequency, the difference in the results becomes large. This too results from the small angle in [12].

V. Conclusion

- Expressions for the transmission properties—the field distribution and reflection and transmission coefficients—on an E-plane and H-plane sector horn junctions in a rectangular waveguide are derived without restrictions on the modal expansion of electromagnetic fields and the flare angle of the horn.
- For $ka/\pi < 2.0$, if the flare angle of the sector horn does not exceed 120°, one may treat only the dominant mode. But for $ka/\pi > 2.0$ or $\phi_0 > 120°$, higher order modes cannot be neglected.
- Generally, as the flare angle increases, the reflection coefficient increases, and for $ka/\pi > 2.0$ the reflection coefficient varies in a complex manner in the case of an H-plane sector horn.
- By expanding the field distribution in the junction to modal functions, investigations of the field distribution in the junction or the radiation directivity from the horn antenna are possible.

References

[1] K. Matsumaru, "Reflection coefficient of E-plane tapered waveguides," *IRE Trans. Microwave Theory Tech.*, vol. MTT-6, pp. 143–149, Apr. 1958.
[2] R. E. Collin, "The optimum tapered transmission line matching section," *Proc. IRE*, vol. 44, pp. 539–548, Apr. 1956.
[3] M. T. Birand and N. Williams, "Input VSWR of profiled E-plane tapers," *Electron. Lett.*, vol. 17, pp. 220–221, Mar. 1981.
[4] L. Lewin, "The E-plane taper junction in rectangular waveguide," *IEEE Trans. Microwave Theory Tech.*, vol. MTT-27, pp. 560–563, June 1979.
[5] A. Chakraborty and G. S. Sanyal, "Transmission matrix of a linear double taper in rectangular waveguides," *IEEE Trans. Microwave Theory Tech.*, vol. MTT-28, pp. 577–579, June 1980.
[6] S. S. Saad, J. B. Davies, and O. J. Davies, "Computer analysis of gradually tapered waveguide with arbitrary cross section," *IEEE Trans. Microwave Theory Tech.*, vol. MTT-25, pp. 437–440, May 1977.
[7] G. Piefke, "Reflexion beim Ubergang vom Rechteck-Hohlleiter zum Sector-Horn," *Arch. Elek. Übertragung.*, vol. 11, pp. 123–135, 1957.
[8] H. Flügel and E. Kühn, "Computer-aided analysis and design of circular waveguide tepers," *IEEE Trans. Microwave Theory Tech.*, vol. 36, pp. 332–336, Feb. 1988.
[9] J. A. Encinar and J. M. Rebollar, "Convergence of numerical solutions of open-ended waveguide by modal analysis and hybrid modal-spectral techniques," *IEEE Trans. Microwave Theory Tech.*, vol. MTT-34, pp. 809–814, July 1986.
[10] L. Lewin, "On the inadequacy of discrete mode-matching techniques in some waveguide discontinuities problems," *IEEE Trans. Microwave Theory Tech.*, vol. MTT-18, pp. 364–372, July 1970.
[11] M. Kosiba, M. Sato, and M. Suzuki, "Finite-element analysis of arbitrarily shaped H-plane waveguide discontinuities," *Trans. IECE Japan*, vol. E66, no. 2, pp. 82–87, Feb. 1983.
[12] F. Sporleder and H.-G. Unger, *Waveguide Tapers, Transitions and Couplers*. London and New York: Peter Peregrinus, 1979, pp. 125–140.

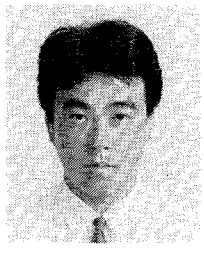

Takashi Tsushima was born in Aomori, Japan, on July 5, 1965. He received the B.E. and M.E. degrees in electrical engineering from Nihon University, Fukushima, Japan, in 1987 and 1989, respectively.

He is now with the Aomori Technical High School.

Mr. Tsushima is a member of the Institute of Electronics, Information and Communication Engineers in Japan.

Shuzo Kuwano (M'77) was born in Fukushima, Japan, on June 14, 1952. He received the B.E. and M.E. degrees in electrical engineering from Nihon University, Fukushima, Japan, in 1975 and 1977, respectively.

He became a Research Assistant in 1977 and an Instructor in 1987 in the Department of Electrical Engineering, College of Engineering, Nihon University. His present research interests include interaction of electromagnetic waves with biological media and numerical techniques in electromagnetics.

Mr. Kuwano is a member of the Institute of Electronics, Information and Communication Engineers in Japan.

Kinchi Kokubun (M'75) was born in Fukushima, Japan, on May 20, 1926. He received the B.E. and D.E. degrees in electrical engineering from Nihon University, Tokyo, Japan, in 1953 and 1974, respectively.

He became an Instructor in 1969, an Associate Professor in 1970, and a Professor in 1975 in the Department of Electrical Engineering, College of Engineering, Nihon University. In July 1990, he became a Dean of the College of Engineering. His professional interests include the areas of microwave passive devices, analysis of waveguide discontinuities, and periodic structures.

Dr. Kokubun is a member of the Institute of Electronics, Information and Communication Engineers in Japan.